Analytic description of neutron star cooling

D. D. Ofengeim* and D. G. Yakovlev

Ioffe Institute, Politekhnicheskaya 26, St Petersburg 194021, Russia

ABSTRACT

We have derived analytic expressions that describe cooling of isolated neutron stars with nucleon cores after reaching the state of internal thermal relaxation. The results are valid for a wide class of equations of state of nucleonic matter and, in this sense, are universal. Moreover, they accurately reproduce the evolution of neutron stars at the neutrino and photon cooling stages as well as during transition from one stage to the other. These results greatly simplify theoretical analysis of internal structure of cooling neutron stars. For illustration, we analyse the thermal state of the bright nearby neutron star RX J1856.5−3754 and present arguments that this star has already left the neutrino cooling stage and contains superfluidity of neutrons and protons inside. We discuss possible efficiency of its neutrino cooling and heat capacity of its core.

Key words: dense matter – equation of state – neutrinos – stars: neutron.

1 INTRODUCTION

Cooling neutron stars have been studied for a long time. Nowadays one knows a few dozens of such stars whose thermal X-ray emissions have been detected and whose ages have been measured or constrained. These observations can be compared with different theoretical scenarios of neutron star cooling for individual stars and for the entire set of objects (e.g. Yakovlev & Pethick 2004; Shternin et al. 2011; Yakovlev et al. 2011; Ofengeim et al. 2015; Page et al. 2015).

It is well known that neutron stars cool via neutrino emission from their body (mainly from the core) and via electromagnetic emission from their surface. For certainty, we restrict ourselves to neutron stars that have nucleon cores neglecting the effects of magnetic fields and possible internal reheating mechanisms. A few decades after its birth, a star becomes isothermal (thermally relaxed) inside, with a strong temperature drop in a thin heat blanketing envelope near the neutron star surface (Gudmundsson, Pethick & Epstein 1983; Potekhin, Chabrier & Yakovlev 1997). With account for general relativity, its redshifted temperature $\widetilde{T}$ in the isothermal region is spacially constant,

$$\widetilde{T} = T \sqrt{g_{00}} = const, \tag{1}$$

where T is the local temperature and g_{00} is the metric tensor component. We will study the temperature evolution $\widetilde{T}(t)$ (t being the star's age) at the cooling stage at which the star is thermally relaxed inside. For about 100 kyr, the star cools mainly via neutrino emission (being at the so-called neutrino cooling stage), and then transits to the photon cooling stage where the cooling is governed by the photon thermal emission. In order to calculate $\widetilde{T}(t)$, one needs to know the total heat capacity C as well as the total neutrino L_ν^∞ and photon L_γ^∞ luminosities of the star (the superscript '∞' marks the quantities measured by a distant observer). To find C and L_ν^∞, one should have a model equation of state (EOS) of stellar matter and models for superfluidities of neutrons and protons. To derive L_γ^∞, one requires a model for a heat blanketing envelope. It relates the effective surface temperature T_s of the star and the temperature T_b at the bottom of the heat blanketing envelope. Then L_γ^∞ is given by

$$L_\gamma^\infty = 4\pi \sigma R^2 T_s^4 (1 - x_g), \tag{2}$$

where σ is the Stefan–Boltzmann constant, $x_g = 2GM/(Rc^2)$, M is the gravitational mass and R the circumferential star's radius. The surface temperature redshifted for a distant observer is $T_s^\infty = T_s\sqrt{1 - x_g}$.

The internal redshifted temperature $\widetilde{T}$ is

$$\widetilde{T} = T_b \sqrt{1 - x_g}. \tag{3}$$

The cooling theory derives the so-called cooling curves (either $T_s^\infty(t)$ or $L_\gamma^\infty(t)$) to be compared with the observations. One has obtained simple analytic $T_s^\infty(t)$ relations at the neutrino and photon cooling stages (e.g. Yakovlev & Pethick 2004; Page et al. 2015 and references therein). They allow one to analyse cooling neutron stars that are either at the neutrino or at the photon cooling stage but not at the transition from one stage to the other.

Here, we obtain an approximate analytic $T_s^\infty(t)$ solution that is valid for the neutrino and photon cooling stages and at the transitional stage as well. Our analysis is based on the analytic approximations of L_ν^∞ and C by Ofengeim et al. (2016), which are nearly universal (valid for different EOSs) and take into account superfluid states of nucleon cores. We will also use the T_s–T_b relations obtained by Potekhin et al. (1997, 2003) and Beznogov, Potekhin & Yakovlev (2016). Our formalism gives a neutron star temperature

* E-mail: ddofengeim@gmail.com

for any age t (after the end of internal thermal relaxation), mass M and radius R.

In order to illustrate possible applications of the new formula, we use it to analyse the internal state of the neutron star RX J1856.5−3754 (Section 4). We will conclude in Section 5, where, in particular, we formulate the applicability conditions of our results and possible extensions of the work.

2 ANALYTIC SOLUTION OF ISOTHERMAL COOLING EQUATIONS

The equation of neutron star cooling after the initial internal thermal relaxation reads

$$C\frac{\mathrm{d}\widetilde{T}}{\mathrm{d}t} = -L_\nu^\infty - L_\gamma^\infty. \tag{4}$$

The neutrino luminosity L_ν^∞ is mainly determined by neutrinos emitted from the stellar core. For most important neutrino emission mechanisms in the core one often has $L_\nu^\infty \propto \widetilde{T}^n$, where $n = 6$ or 8 (see, e.g. Yakovlev et al. 2001 for details). Since the heat capacity of the star is also mainly provided by the core and $C \propto \widetilde{T}$, we can set

$$\frac{L_\nu^\infty}{C} = \zeta q \widetilde{T}_9^{n-1}, \tag{5}$$

where $\zeta = (10^9 \text{ K})/(1 \text{ yr}) \approx 31.69 \text{ K s}^{-1}$ and $\widetilde{T}_9 = \widetilde{T}/(10^9 \text{ K})$. The dimensionless neutrino cooling factor q depends only on the mass of the star and on the EOS model.

One can obtain a similar expression for L_γ^∞/C but under additional simplifications. It is well known (e.g. Page et al. 2015) that a T_s–T_b relation can often be approximated by a simple power law,

$$T_{s6}^4 = a g_{14} T_{b9}^\alpha, \tag{6}$$

where g_{14} is a surface gravity expressed in $10^{14} \text{ cm s}^{-2}$, $T_{s6} = T_s/(10^6 \text{ K})$ and $T_{b9} = T_b/(10^9 \text{ K})$. The scaling relation $T_s^4 \propto g$ is well justified (Gudmundsson et al. 1983); a and α can be extracted, e.g. from accurate T_s–T_b fits by Potekhin et al. (1997, 2003) and Beznogov et al. (2016). Here, we consider T_s–T_b relations that are similar to the model by Gudmundsson et al. (1983), for which $\alpha \approx 2$. Combining equations (2) and (3), we get

$$\frac{L_\gamma^\infty}{C} = \zeta s \widetilde{T}_9^{\alpha-1}, \tag{7}$$

where s is approximately constant; it can be called a dimensionless photon cooling factor. Equation (7) can be used to calculate s.

Now the cooling equation (4) can be rewritten as

$$\frac{\mathrm{d}\widetilde{T}_9}{\mathrm{d}t_{\mathrm{yr}}} = -q\widetilde{T}_9^{n-1} - s\widetilde{T}_9^{\alpha-1}, \tag{8}$$

where $t_{\mathrm{yr}} = t/(1 \text{ yr})$. Its formal solution is

$$t_{\mathrm{yr}} - t_{0\mathrm{yr}} = \int_{\widetilde{T}_9}^{\widetilde{T}_{09}} \frac{\mathrm{d}\widetilde{T}_9'}{q\widetilde{T}_9'^{n-1} + s\widetilde{T}_9'^{\alpha-1}}. \tag{9}$$

It is assumed here that the redshifted temperature is equal to $\widetilde{T}_0$ at some initial moment of time t_0. One can express t_{yr} through a dimensionless integral

$$t_{\mathrm{yr}} - t_{0\mathrm{yr}} = \frac{1}{q(n-2)}\left(\frac{q}{s}\right)^k \int_{x_0}^x \frac{\mathrm{d}y}{y^{1/k}+1}, \quad x = \left(\frac{s}{q}\right)^k \widetilde{T}_9^{2-n}, \tag{10}$$

where $k = (n-2)/(n-\alpha)$ and $x_0 = x\big|_{\widetilde{T}_{09}}$.

At the next step let us focus on the important case of $t \gg t_0$ and $\widetilde{T}_0^{n-2} \gg \widetilde{T}^{n-2}$. Then the initial condition becomes forgotten (see, e.g. Yakovlev et al. 2011; Shternin & Yakovlev 2015). In this case, introducing

$$I_\beta(x) = \int_0^x \frac{\mathrm{d}y}{y^\beta + 1}, \tag{11}$$

from equation (10) we get

$$t_{\mathrm{yr}}\left(\widetilde{T}_9\right) = \frac{1}{(n-2)q}\left(\frac{q}{s}\right)^k I_{1/k}\left(\frac{(s/q)^k}{\widetilde{T}_9^{n-2}}\right). \tag{12}$$

At first, let us discuss the case of $\alpha = 2$. It leads to $\beta = 1$ in equation (11), $I_1(x) = \ln(1+x)$ and to the cooling curve

$$\widetilde{T}_9(t_{\mathrm{yr}}) = \left[\frac{s/q}{\exp\left\{(n-2)st_{\mathrm{yr}}\right\}-1}\right]^{1/(n-2)}. \tag{13}$$

At the neutrino cooling stage, $st_{\mathrm{yr}} \ll 1$, one gets the well known expression $\widetilde{T}_9 = [(n-2)qt_{\mathrm{yr}}]^{1/(n-2)}$ (e.g. Yakovlev et al. 2011). At the photon cooling stage, $st_{\mathrm{yr}} \gg 1$, equation (13) reduces to the expression $\widetilde{T}_9 = (s/q)^{1/(n-2)} \exp(-st_{\mathrm{yr}})$ given, for instance, by Page et al. (2015). However, the latter authors have not presented a cooling equation valid at the transition between the neutrino and photon cooling stages.

For many realistic models of heat blanketing envelopes, we have $|\alpha - 2| \lesssim 0.2$. Even in the case of fast direct Urca cooling, $n = 6$ (Yakovlev & Pethick 2004), such values of α give $|\beta - 1| \lesssim 0.05$. Accordingly, we can use the approximation

$$I_\beta(x) \approx \frac{(x+1)^{1-\beta}-1}{1-\beta}. \tag{14}$$

For the indicated values of β, its accuracy is good, and the relative error does not exceed 3 per cent (as can be checked by direct calculation). One can combine equations (14) with (12) and get

$$\widetilde{T}_9(t_{\mathrm{yr}}) = \left[\frac{(s/q)^k}{\left((\alpha-2)s^k q^\gamma t_{\mathrm{yr}}+1\right)^{-k/\gamma}-1}\right]^{1/(n-2)}, \tag{15}$$

where $\gamma = (2-\alpha)/(n-\alpha)$. This formula allows one to determine the redshifted temperature of the star at both the neutrino and photon cooling stages. One just needs to know the cooling factors q and s (Section 3). Note that equation (15) is easily inverted to obtain t_{yr} as a function of $\widetilde{T}_9$.

Let us outline some properties of the new formula. First, it reproduces the simple relation (13) in the limit $\alpha \to 2$. Then, for small t (neutrino cooling) it gives true $\widetilde{T}(t)$ for any α. In the opposite case of large t (photon cooling) equation (15) reads

$$\widetilde{T}_9(t_{\mathrm{yr}}) \approx \left(\frac{s}{q}\right)^{1/(n-\alpha)} \left[(\alpha-2)s^k q^\gamma t_{\mathrm{yr}}+1\right]^{1/(2-\alpha)}. \tag{16}$$

In the limit $\alpha \to 2$, it gives the same expression as the photon cooling limit of equation (13). Note that at $\alpha < 2$ equations (15) and (16) give a non-physical result, according to which $\widetilde{T}$ drops to zero at a finite t. However, it is not a fatal disadvantage of our approach, as the T_s–T_b relation (6) with $\alpha \sim 2$ works only in the temperature range of $T_b \gtrsim 3 \times 10^6$ K (Potekhin et al. 2003). At the later cooling stage, the T_s–T_b relation has to be modified but a star becomes so cold that it is not observable even with the best currently available detectors. Therefore, equation (15) is valid for exploring observable cooling neutron stars.
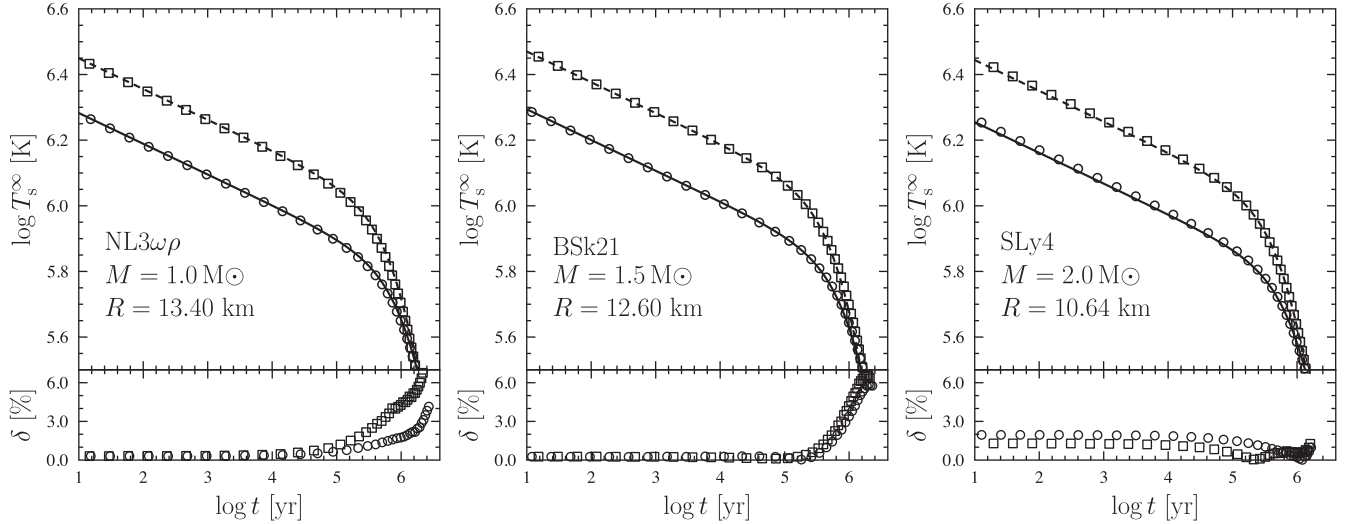
Figure 1. Cooling curves for three neutron star models with iron heat blanketing envelopes. Circles and squares are numerical solutions of equation (4) with modified Urca process (no proton superfluidity) and neutron–neutron collisions (fully superfluid protons) as the leading neutrino cooling mechanisms, respectively. Solid and dashed lines are the analytic approximations (15) for the same models. Lower panels display absolute values of relative errors of the analytic approximations. See text for details.

3 MATCHING WITH NUMERICAL COOLING SIMULATIONS

To test our approximate analytic solution (15), we have solved the cooling equation (4) numerically for three selected neutron star models with different masses and EOSs. For all of them, we have used the iron heat blanketing envelopes with the T_s–T_b relation derived by Potekhin et al. (1997). The results are plotted in Fig. 1. The left-hand panel is for a 1 M$_\odot$ neutron star with the NL3$\omega\rho$ EOS (Fortin et al. 2016); this is an example of a relativistic mean field EOS. The second panel corresponds to a 1.5 M$_\odot$ star with the BSk21 EOS (e.g. Potekhin et al. 2013). Finally, the right-hand side panel is for a 2.0 M$_\odot$ star with the SLy4 EOS (Douchin & Haensel 2001). The latter two EOSs belong to the family of modified Skyrme EOSs. The selected neutron star models each have a different compactness and average density that are the main regulators of L_ν^∞ and C. The NL3$\omega\rho$ 1 M$_\odot$ star is less compact and cools most slowly at the neutrino cooling stage, while the SLy4 2 M$_\odot$ star is rather compact and cools faster.

In all the three neutron star models in Fig. 1, the most powerful direct Urca process of neutrino cooling (Lattimer et al. 1991) is forbidden. For each star, we consider two leading neutrino cooling mechanisms. In the first case, we neglect possible superfluidity of nucleons in neutron stars; then the leading neutrino emission is provided by the modified Urca process. In the second case, we assume strong proton superfluidity throughout the stellar core that suppresses all neutrino mechanisms involving protons as well as the proton heat capacity. Then the leading neutrino emission is produced by a weaker neutrino-pair bremsstrahlung due to neutron–neutron collisions; a star cools slower than in the non-superfluid case. Exact solutions of equation (4) for non-superfluid stars are shown by open circles, while the exact solutions for stars with strong proton superfluidity are shown by open squares. Corresponding approximate analytic cooling solutions (15) are displayed by solid and dashed lines, respectively.

To construct these approximate solutions $T_s^\infty(t)$, one needs to find a and α in equation (6) for the chosen heat blanketing envelope, and to calculate q and s in equations (5) and (7). We have verified

that the T_s–T_b fits derived by Potekhin et al. (1997) for the iron heat blanketing envelope can be approximated by equation (6) with $a = 73$ and $\alpha = 2.2$. In the range of $T_b = 10^7 - 10^9$ K, this approximation has the relative root mean square error ∼3 per cent, with the maximal error ∼7 per cent at the lowest T_b. We note that we do not recommend calculating $T_s^\infty(t)$ by combining (6) and (15); one should better use the T_s–T_b relations by Potekhin et al. (1997) or Beznogov et al. (2016) to avoid extra inaccuracies. To get q and s, we have used the approximations of Ofengeim et al. (2016) for L_ν^∞ and C. These approximations and equation (2) allow one to treat q and s as independent functions of M and R. Such an approach makes our approximate cooling curves valid for a wide class of nucleonic EOSs in neutron star cores (see Ofengeim et al. 2016 for details). In particular, we have checked that these approximations are valid for the APR EOS (Akmal, Pandharipande & Ravenhall 1998), which has not been used for deriving the approximations.

The agreement between the exact and approximate cooling curves in Fig. 1 is impressive. This is additionally confirmed by the curves at the bottom panels of Fig. 1, which display absolute values of relative deviations δ between exact and approximate solutions $T_s^\infty(t)$. For 1 and 1.5 M$_\odot$ neutron stars, our approximation reproduces the neutrino cooling stage almost exactly and has $\delta \lesssim 7$ per cent during the photon cooling stage. The reason for the growing inaccuracy in an older star is the lack of a simple and accurate T_s–T_b relation (6) at low temperatures. For massive stars (the right-hand panel of Fig. 1), we have the opposite situation; the $L_\nu^\infty(\widetilde{T})$ approximations by Ofengeim et al. (2016) have the worst accuracy for $M \gtrsim 2$ M$_\odot$. However, they lead to relatively small inaccuracies $\delta \sim (2$–3) per cent of the cooling curves at both cooling stages.

4 THERMAL STATE OF RX J1856.5−3754

RX J1856.5−3754 (hereafter RX J1856) was identified as an isolated neutron star by Walter, Wolk & Neuhäuser (1996). It is one of the brightest thermally emitting nearby neutron stars; it belongs to the group of neutron stars called 'The Magnificent Seven' (Haberl 2007). Ho et al. (2007) successfully fitted its spectrum by
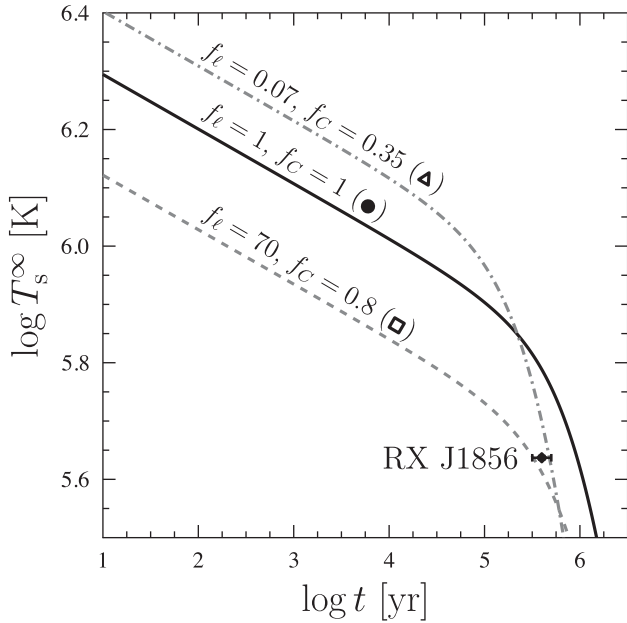
Figure 2. Cooling curves compared to the measured temperature and age of RX J1856 (the diamond with error bars) obtained assuming $M = 1.48$ M$\odot$ and $R = 12.1$ km (Potekhin 2014) and using equation (15). The curves are marked by the values of two dimensionless parameters (17). Cooling of the 'standard neutrino candle' (black solid line) makes RX J1856 too warm. The grey dashed and dash–dotted lines display two cooling models modified by superfluidity; they are consistent with the observations. The symbols in brackets mark cooling scenarios (the same as in Fig. 3). See text for details.

Figure 3. Possible values of the cooling factors (17), f_ℓ and f_C, for RX J1856. The double-hatched strip is the restriction from the observational ranges of T_s^∞ and t. The filled circle corresponds to the 'standard neutrino candle' (the solid cooling curve in Fig. 2). The open square and triangle refer to an enhanced cooling with $f_\ell = 70$, $f_C = 0.8$ and to a slow cooling with $f_\ell = 0.07$, $f_C = 0.35$, respectively (the dashed and dash–dotted cooling curves in Fig. 2). The single-hatched area is the (f_ℓ, f_C) domain for RX J1856 with non-superfluid neutrons and party superfluid protons. The dark shaded regions A–D are forbidden for various reasons explained in the text.

a model of a thin magnetic hydrogen atmosphere on top of a condensed iron surface with $T_s^\infty = (4.34 \pm 0.03) \times 10^5$ K (as detailed by Potekhin 2014). Walter et al. (2010) refined parallax distance measurements to RX J1856 (123^{+11}_{-15} pc at 1σ level), that allowed Potekhin (2014) to constrain mass and radius of the neutron star, $M = 1.48^{+0.16}_{-0.19}$ M$\odot$, $R = 12.1^{+1.3}_{-1.6}$ km. The age of RX J1856 is not very certain. Here, we adopt the age range, $\log t_{yr} = 5.5 - 5.7$, given by Viganò et al. (2013). Fig. 2 displays observational cooling properties of RX J1856 in the $T_s^\infty - t$ plane.

Here, we adopt the interpretation of the RX J1856 spectrum mentioned above (condensed iron surface under a thin hydrogen atmosphere). Then we can assume a fully iron heat blanketing envelope of the star and employ the T_s–T_b relation given by Potekhin et al. (1997). Therefore, we can use the simple $\widetilde{T}(t)$ solution (15) to analyse the RX J1856 cooling.

Fig. 2 shows three cooling curves obtained from equations (2), (3) and (15) for $M = 1.48$ M$\odot$ and $R = 12.1$ km (see above). The solid cooling curve corresponds to a 'standard neutrino candle' (Yakovlev et al. 2011), which is a non-superfluid star where the direct Urca process is forbidden. Its neutrino cooling goes mainly though the modified Urca process. Solid lines in Fig. 1 are derived in the same way but for different values of M and R. According to Fig. 2, RX J1856 cannot be the 'standard neutrino candle' (under the formulated assumptions). However, the data can be explained by deviations from the standard candle that can be caused by superfluidity in the neutron star core.

Recall that for several leading neutrino cooling mechanisms (e.g. Gusakov et al. 2004; Page et al. 2004), the neutrino luminosity of a superfluid star has the same temperature dependence as for a
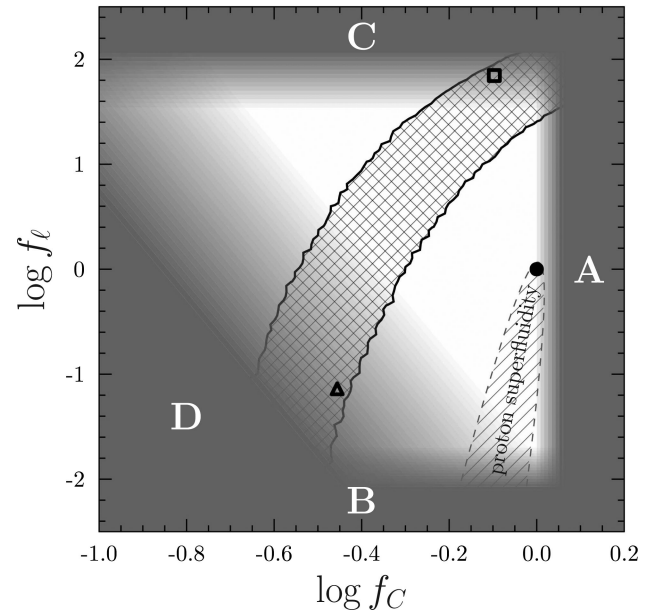
'standard neutrino candle,' $L_\nu^\infty \propto \widetilde{T}^8$. It is instructive to introduce two dimensionless factors,

$$f_\ell = \frac{L_\nu^\infty/C}{L_{\nu\,SC}^\infty/C_{SC}} = \frac{q}{q_{SC}} \quad \text{and} \quad f_C = \frac{C}{C_{SC}} = \frac{s_{SC}}{s}. \quad (17)$$

Here, $L_{\nu\,SC}^\infty$, C_{SC}, q_{SC} and s_{SC} correspond to the 'standard neutrino candle,' while L_ν^∞, C, q and s are actual values that deviate from the standard candle ones. The factor f_ℓ has been introduced before (e.g. Yakovlev et al. 2011) and has been called the dimensionless neutrino cooling function. It is the ratio of L_ν^∞/C (which regulates neutron star cooling at the neutrino cooling stage) to the corresponding ratio for the standard candle. The factor f_C is the ratio of the heat capacity of the given star to the heat capacity of the standard candle (i.e. of the non-superfluid star with the same M and R). It can be called the heat capacity function. It has not been introduced before because it has no direct effect on cooling at the neutrino cooling stage. Since we consider both (the neutrino and photon) cooling stages, we should introduce both factors (17) to specify the cooling curves.

Standard neutrino candle cooling corresponds to $f_\ell = 1$ and $f_C = 1$. The factor f_ℓ governs the neutrino cooling stage (e.g. Weisskopf et al. 2011; Yakovlev et al. 2011), since the corresponding limit of equation (15) does not contain s. The photon cooling stage involves both q and s and is thus regulated by both factors.

Let us outline physical effects that influence neutron star cooling (see Page et al. 2015, for a comprehensive review). The heat capacity is affected by neutron and proton superfluidities in a similar way. If a local $T \lesssim T_c$, where T_c is a local critical temperature for some pairing type, the specific heat is slightly enhanced but it becomes suppressed with the further drop of T. As a result, the total heat capacity is either slightly enhanced (f_C can barely exceed 1.1) or suppressed. In Fig. 3, which displays the f_ℓ–f_C plane, the right-hand-side dark-grey area A

roughly corresponds to the f_C restrictions described above. Different models of pairing gaps change upper bounds on f_C. That is why we smooth out the boundary of the forbidden domain.

However, the total heat capacity C cannot be lower than its electron contribution. As a result, one has $f_C \gtrsim 0.06$–0.1; accordingly, we display the f_C axis in Fig. 3 for $f_C > 0.1$.

The neutrino cooling factor f_ℓ can drastically deviate from $f_\ell = 1$ due to a strong superfluid suppression or enhancement of L_ν^∞. Moreover, neutron and proton pairings affect the neutrino emission in the opposite ways. Proton $^1S_0$ pairing (if it occurs in a neutron star core) can exponentially suppress all neutrino emission processes involving protons. The strongest suppression of the modified Urca (MU) process, is $L_{\nu\,nn}^\infty / L_{\nu\,MU}^\infty \sim 0.01$, where $L_{\nu\,nn}^\infty$ is the neutrino luminosity owing to neutron–neutron collisions and $L_{\nu\,MU}^\infty$ is the luminosity provided by the MU process (both luminosities were approximated by Ofengeim et al. 2016). Different EOSs give different strongest suppressions; this restriction is displayed on Fig. 3 by the lower dark horizontal strip B with a smooth upper bound.

The single-hatched region qualitatively represents an (f_ℓ, f_C) domain for a star with non-superfluid neutrons. The region starts from the 'standard neutrino candle' point (the black circle, $f_\ell = f_C = 1$) and spreads down to the lower bound of f_ℓ slightly declining from the vertical direction $f_C = const$, because proton pairing gradually reduces the proton heat capacity. In contrast, neutron $^3(P - F)_2$ pairing, whose appearance in the stellar core is also expected, enhances the neutrino luminosity due to Cooper pairing (CP) neutrino emission, which is especially strong for this pairing type; e.g. Leinson & Pérez (2006); Page et al. (2009) and references therein. In this way f_ℓ can be as high as ~ 100. Different models of neutron superfluidity lead to different maximal values of f_ℓ, and we approximately show this restriction by the upper dark strip C with smoothed out lower bound.

The CP neutrino emission switches on sharply when the temperature T falls below the maximum value of T_{cn} in the stellar core. When the star cools further, f_ℓ stays approximately constant and can be as high as ~ 100 or much lower depending on the stellar mass M and neutron critical temperature profile $T_{cn}(\rho)$ in the core (e.g. Page et al. 2004; Gusakov et al. 2004; Page et al. 2009). Many neutron superfluidity models, which are thought to be realistic, have characteristic $T_{cn}(\rho)$ profiles that imply the presence of non-superfluid neutrons at least somewhere in the core. If f_C is less than the minimal value that proton pairing can provide, then one can expect some neutron pairing in the core, i.e. the neutrino luminosity can be enhanced by the CP neutrino emission. Accordingly, for small f_C there should be some minimal f_ℓ that grows up when f_C decreases. Such a relation between the minimal f_ℓ and f_C should depend on pairing models. In any case, it should prohibit the left-hand bottom corner in Fig. 3. This corner is displayed as the dark area D; since we do not know the exact boundary of the prohibited area, the darkening is smoothed out. In any case, this domain disappears with growing f_ℓ and/or f_C.

Strictly speaking, f_ℓ and f_C can vary with time as the star cools. However, RX J1856 is sufficiently cold so that f_ℓ and f_C are expected to be 'frozen', almost independent of time, which justifies our consideration. In this case, any cooling curve in Fig. 2 is equivalent to some point in the f_ℓ–f_C plane (Fig. 3). For example, we have chosen two (f_ℓ, f_C) points that are consistent with the RX J1856 observations. One point corresponds to a slow neutrino cooling ($f_\ell = 0.07, f_C = 0.35$, the triangle on Fig 3), while the second one to the enhanced neutrino cooling ($f_\ell = 70, f_C = 0.8$, the square on Fig. 3). Corresponding cooling curves are plotted in Fig. 2 by the dash–dotted and dashed lines. In the first case, the neutrino cooling is slow but the heat capacity is noticeably lower than for the standard neutrino candle. Because of lower heat content, RX J1856 leaves the neutrino cooling stage more quickly (than the standard neutrino candle) and then cools faster via photon surface emission; in this way the cooling curve hits the observational error box. In the second case, the star cools faster through the CP neutrino emission at the neutrino cooling stage, but its heat capacity is almost the same as for the standard neutrino candle. Then the neutrino cooling stage is delayed with respect to the first case, but once the photon surface emission becomes important, the cooling curve also hits the observational error box.

Which area of the f_ℓ–f_C plane is appropriate for RX J1856? To answer this question we have selected a grid of f_ℓ and f_C values, with $\log f_\ell$ from -2.5 to 2.5 and $\log f_C$ from -1.0 to 0.2. For each (f_ℓ, f_C) point of this grid, we have checked if there exists any t in the RX J1856 age error box that gives T_s^∞ in the observational error box for RX J1856. The points satisfying this condition constitute the double-hatched domain in Fig. 3. Any point from this domain represents a formal solution of the cooling problem (and is formally consistent with the observations of RX J1856). As expected, both the open triangle and open square lie within this domain (but in its opposite corners).

Note that this domain remains nearly the same if we use the photon cooling limit (16) instead of the full solution (15). This indicates that RX J1856 has already passed the neutrino cooling stage.

However, one should distinguish between formal and realistic solutions. In our case, it is reasonable to consider the solutions in the dark areas of Fig. 3 as unrealistic (see above). Therefore, the realistic solutions belong to the non-darkened area of the double-hatched region, with the centre at $\log f_\ell \approx 1$ and $\log f_C \approx -0.3$. This area is still too wide to greatly constrain f_ℓ and f_C. It contains many different solutions, but nevertheless restricts f_ℓ and f_C. Note that the domain of realistic solutions does not intersect the single-hatched domain that corresponds to RX J1856 with non-superfluid neutrons. This means that our realistic cooling solutions favour for RX J1856 models with essentially both proton and neutron superfluidities.

Having the family of realistic values of f_ℓ and f_C, at the next step one can try to find realistic physical models for neutron and proton superfluidities [corresponding profiles of critical temperatures, $T_{cn}(\rho)$ and $T_{cp}(\rho)$] that result in these f_ℓ and f_C. This is a difficult problem, which is beyond the scope of the present work. One can expect that realistic solutions would imply strong proton superfluidity in an appreciable part of the neutron star core as well as moderate neutron superfluidity whose $T_{cn}(\rho)$ profiles resemble those predicted for the neutron star in the Cas A supernova remnant (Page et al. 2011; Shternin et al. 2011; Shternin & Yakovlev 2015).

5 CONCLUSIONS

We have derived an approximate analytic expression (Sections 2 and 3) for cooling curves $T_s^\infty(t)$ of isolated neutron stars after they reach the state of internal thermal relaxation (a few decades after their birth). The expression is equally valid at the neutrino and photon cooling stages as well as at the transition from one stage to the other at $t \sim 10^5$ yr. It is obtained for a wide class of EOSs of nucleon matter in neutron star cores (the same EOSs as used in Ofengeim et al. 2016). The expression depends on the mass and radius of the star and on superfluid properties of neutron star cores but it is one and the same for all EOSs. From this point of view, it is universal and allows one to perform a simple and almost model-independent theoretical interpretation of thermal states of observed isolated

neutron stars. We have started to develop such a model-independent analysis (Yakovlev et al. 2011; Weisskopf et al. 2011; Shternin & Yakovlev 2015; Klochkov et al. 2015; Ofengeim et al. 2015, 2016); this paper extends previous considerations to the photon cooling stage.

To illustrate the efficiency of this method, we have analysed (Section 4) possible thermal states of the nearby thermally emitting neutron star RX J1856, taking the observables (M, R, T_s^∞ and t) from the literature (Ho et al. 2007; Walter et al. 2010; Potekhin 2014; Viganò et al. 2013). We have assumed that the strongest direct Urca neutrino process does not operate in RX J1856. It is convenient to specify a thermal state of RX J1856 by the two dimensionless cooling parameters (17), f_ℓ and f_C, which determine the neutrino cooling function and heat capacity of the star in terms of the same quantities for a standard neutrino candle (e.g. Yakovlev et al. 2011). These two parameters seem to realize a general description of cooling isolated neutron stars; they can be extracted from observations using our analytic expressions, and they are good for comparing internal structures of different cooling neutron stars. In the case of RX J1856, a possible domain of f_ℓ and f_C is plotted in Fig. 3 as the non-darkened part of the double-hatched region. Our analysis indicates that RX J1856 has already passed the neutrino cooling stage and the stellar core contains both neutron and proton superfluidities.

Let us stress that even if we could accurately pinpoint f_ℓ and f_C for some star, this would not mean a complete determination of the physical state of the stellar interior because one and the same f_ℓ and f_C can be realized by a number of physical models. Nevertheless, one can try to restrict a real physical model at a later stage, taking into account other observational data.

The presented results should be treated as preliminary, as a sketch of a model-independent analysis of internal states of cooling neutron stars to be elaborated in the future. The current state of the affair is not complete. For instance, our analytic approximations of L_ν^∞ and C are obtained using simplified expressions for the neutrino emissivities in different neutrino reactions assuming fixed effective masses of nucleons in the stellar cores (as described, e.g. by Ofengeim et al. 2016). So far we have not included the effects of magnetic fields on the neutron star cooling, and we have not considered neutron stars that can be additionally heated inside like magnetars (e.g. Kaminker et al. 2009; Pons & Rea 2012). While applying our results, we have used the models of heat blanketing envelopes consisting of pure iron; more complicated composition of these envelopes needs a more careful analysis of analytic approximations. Finally, we warn the readers against applying our formulae to old and cold neutron stars (say, $T_s \lesssim 10^5$ K) because the T_s–T_b relations for these stars (whose thermal surface emission is very difficult to detect) are still far from being perfect because of many theoretical obstacles like partial ionization and the effects of non-ideal plasma, as reviewed by Potekhin (2014).

REFERENCES

Akmal A., Pandharipande V. R., Ravenhall D. G., 1998, Phys. Rev. C, 58, 1804
Beznogov M. V., Potekhin A. Y., Yakovlev D. G., 2016, MNRAS, 459, 1569
Douchin F., Haensel P., 2001, A&A, 380, 151
Fortin M., Providência C., Raduta A. R., Gulminelli F., Zdunik J. L., Haensel P., Bejger M., 2016, Phys. Rev. C, 94, 035804
Gudmundsson E. H., Pethick C. J., Epstein R. I., 1983, ApJ, 272, 286
Gusakov M. E., Kaminker A. D., Yakovlev D. G., Gnedin O. Y., 2004, A&A, 423, 1063
Haberl F., 2007, Ap&SS, 308, 181
Ho W. C. G., Kaplan D. L., Chang P., van Adelsberg M., Potekhin A. Y., 2007, Ap&SS, 308, 279
Kaminker A. D., Potekhin A. Y., Yakovlev D. G., Chabrier G., 2009, MNRAS, 395, 2257
Klochkov D., Suleimanov V., Pühlhofer G., Yakovlev D. G., Santangelo A., Werner K., 2015, A&A, 573, A53
Lattimer J. M., Pethick C. J., Prakash M., Haensel P., 1991, Phys. Rev. Lett., 66, 2701
Leinson L. B., Pérez A., 2006, Phys. Lett. B, 638, 114
Ofengeim D. D., Kaminker A. D., Klochkov D., Suleimanov V., Yakovlev D. G., 2015, MNRAS, 454, 2668
Ofengeim D. D., Fortin M., Haensel P., Yakovlev D. G., Zdunik J. L., 2016, preprint (arXiv:1612.04672)
Page D., Lattimer J. M., Prakash M., Steiner A. W., 2004, ApJS, 155, 623
Page D., Lattimer J. M., Prakash M., Steiner A. W., 2009, ApJ, 707, 1131
Page D., Prakash M., Lattimer J. M., Steiner A. W., 2011, Phys. Rev. Lett., 106, 081101
Page D., Lattimer J. M., Prakash M., Steiner A. W., 2015, in Bennemann K. H., Ketterson J. B., eds, Novel Superfluids vol. 2, Vol. 157. Oxford Univ. Press, Oxford, p. 505
Pons J. A., Rea N., 2012, ApJ, 750, L6
Potekhin A. Y., 2014, Phys.-Usp., 57, 735
Potekhin A. Y., Chabrier G., Yakovlev D. G., 1997, A&A, 323, 415
Potekhin A. Y., Yakovlev D. G., Chabrier G., Gnedin O. Y., 2003, ApJ, 594, 404
Potekhin A. Y., Fantina A. F., Chamel N., Pearson J. M., Goriely S., 2013, A&A, 560, A48
Shternin P. S., Yakovlev D. G., 2015, MNRAS, 446, 3621
Shternin P. S., Yakovlev D. G., Heinke C. O., Ho W. C. G., Patnaude D. J., 2011, MNRAS, 412, L108
Viganò D., Rea N., Pons J. A., Perna R., Aguilera D. N., Miralles J. A., 2013, MNRAS, 434, 123
Walter F. M., Wolk S. J., Neuhäuser R., 1996, Nature, 379, 233
Walter F. M., Eisenbeiß T., Lattimer J. M., Kim B., Hambaryan V., Neuhäuser R., 2010, ApJ, 724, 669
Weisskopf M. C., Tennant A. F., Yakovlev D. G., Harding A., Zavlin V. E., O'Dell S. L., Elsner R. F., Becker W., 2011, ApJ, 743, 139
Yakovlev D. G., Pethick C. J., 2004, ARA&A, 42, 169
Yakovlev D. G., Kaminker A. D., Gnedin O. Y., Haensel P., 2001, Phys. Rep., 354, 1
Yakovlev D. G., Ho W. C. G., Shternin P. S., Heinke C. O., Potekhin A. Y., 2011, MNRAS, 411, 1977

This paper has been typeset from a TEX/LATEX file prepared by the author.